



ELSEVIER

Thermochimica Acta 249 (1995) 249–258

---

---

thermochimica  
acta

---

---

## Spectroscopic and thermal studies on 1,4,5,8-tetranitro tetraaza decalin (TNAD)

K.V. Prabhakaran<sup>1</sup>, N.M. Bhide, E.M. Kurian \*

*Explosives Research and Development Laboratory, Pashan, Pune-411 021, India*

Received 19 January 1994; accepted 27 June 1994

---

### Abstract

TNAD, a polycyclic nitramine, has been studied with regard to the kinetics and mechanism of thermal decomposition and also the morphology and the gaseous products evolved therefrom, using thermogravimetry (TG), differential thermal analysis (DTA), infrared (IR) spectroscopy, differential scanning calorimetry (DSC) and hot stage microscopy. The IR spectra of TNAD have also been recorded and the bands assigned. The kinetics of thermolysis have been followed by isothermal TG. The best linearity (with a correlation coefficient of 0.9859) has been obtained for the three dimensional diffusion controlled equation. The activation energy has been found to be 156.48 kJ mol<sup>-1</sup> and log(*A/s*<sup>-1</sup>) is 13.77. The effect of a series of additives incorporated to the extent of 5%, on the initial thermolysis of TNAD, has also been studied. Evolved gas analysis by IR spectroscopy showed that CO<sub>2</sub>, NO<sub>2</sub>, NO and N<sub>2</sub>O are produced in larger amounts than CO and HCN. The cleavage of the N–N bond appears to be the primary step in the thermolysis of TNAD.

*Keywords:* Decomposition; EGA; IRS; Kinetics; Mechanism; Polycyclic nitramine; TA

---

### 1. Introduction

Development of energetic materials with improved crystal density and high stored energy is underway to meet superior performance requirements. Of the many trends towards this end, one is centred around compounds with higher density and very

---

\* Corresponding author.

<sup>1</sup> Present address: Armament Research and Development Establishment, Pashan, Pune-21, India.

high detonation velocity to meet the ever increasing demand for more energy. In this class one finds the three dimensional caged nitro compounds and the polycyclic polynitramines [1,2]. These compounds have an optimum number of nitro groups, high crystal density and high strain energies. The ongoing research work on the synthesis of such compounds is based on the fact that they are more dense than their open structure counterparts and their higher density results in higher detonation velocity (VOD), because the VOD increases in proportion to the square of the density. The reported synthesis of TNAD [3], *trans*-1,3,5,7-tetranitro glycoluril [4] and 1,4-dinitro cubanes [2] are the result of efforts in this direction. They appear to be the future candidates to compete with the currently used high performance high energy materials such as cyclo trimethylene trinitramine (RDX) and cyclo tetramethylene tetranitramine (HMX) [5,6]. There is a strong dependence between pressure and the thermal decomposition [7,8] and the heat of explosion of TNAD is  $5.639 \text{ kJ g}^{-1}$  [9]. It is also reported that the shock sensitivity of this compound [10] is related to the bond strength [11,12] of the nitramino group. Yinon [13], using MS/MS collision induced dissociation studies, was able to show the fragmentation process and paths in a series of commonly used energetic materials which included nitramines. Nikishev et al. [14] are of the opinion that the reactivity of the nitramines in homolytic thermoanalysis is governed by the closeness of the electronic structure of the reaction centre in ground and transition states. However no data are available regarding the kinetics and mechanism of the thermal decomposition of this compound or its structural aspects, so the present paper is an effort to increase our knowledge in this direction.

## 2. Experimental

TNAD was prepared in gram batches in the laboratory by reported methods [3]. EGA was carried out using a specially designed IR gas cell of path length 10 cm fabricated from pyrex glass using prepelletted spectroscopic grade KBr windows under atmospheric pressure. The sample was heated at a programmed heating rate in a pyrex glass tube which was coupled to the gas cell in such a way that the heated zone and the gas cell were sufficiently apart to prevent any condensed residue reaching the cell windows. Further experimental details have been given in our previous paper [15].

## 3. Results

### 3.1. IR studies

The IR spectrum is reproduced in Fig. 1. The IR spectral assignments are rather straightforward (Table 1). The symmetric nitro stretching modes are multiplets (quartets). The N–NO<sub>2</sub> band can easily be identified by its characteristic stretching absorption at  $1555 \text{ cm}^{-1}$ . The CH<sub>2</sub> scissoring modes are unusually weak at  $1410\text{--}1460 \text{ cm}^{-1}$  although the CH<sub>2</sub> wagging modes are fairly strong.

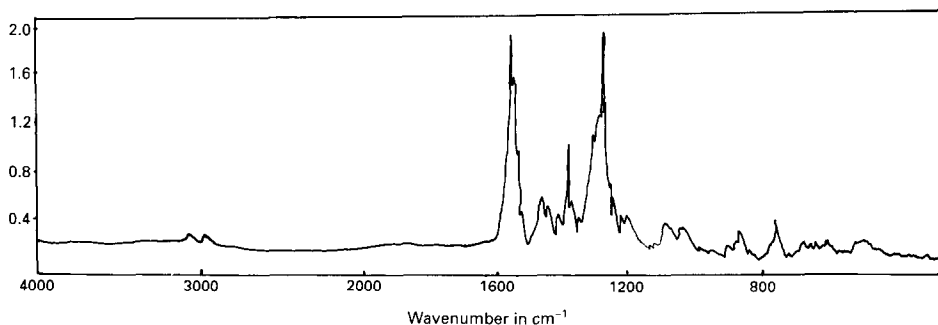


Fig. 1. IR spectra of TNAD.

Table 1  
IR spectral assignments of TNAD

Wavenumber/cm <sup>-1</sup>	Assignment
3040w 2980w	CH <sub>2</sub>
1555vs	N–NO <sub>2</sub> asymmetric
1460w 1430w	δCH <sub>2</sub> scissoring
1410w	
1360m	δCH <sub>2</sub> wagging
1290vs 1240s	N–NO <sub>2</sub> symmetric
1210s 1190s	
1120m 1075s	Ring
1030s	
980w 890w	CH <sub>2</sub> rocking
860m	
835w	
770w 750s	Ring
685w	δNO <sub>2</sub>

Key: m, medium; s, sharp; sh, shoulder; w, weak; vs, very strong.

### 3.2. Thermal decomposition studies

TG/DTA curves of TNAD (Fig. 2) were recorded under different conditions. The TG of TNAD in static air at a heating rate of 10°C min<sup>-1</sup> showed a sharp change in mass of 75% followed by a very slow change in mass of 17%. These mass changes occurred in the temperature ranges 192–220°C and 220–512°C, respectively. The results obtained were similar when the atmosphere was changed to dynamic nitrogen. When the heating rate was changed to 5 and 2°C min<sup>-1</sup>, the initial mass loss was observed at the lower temperature ranges of 189–205°C and 183–197°C, respectively.

DTA of TNAD (Fig. 2) showed two sharp exotherms in the temperature ranges 209–252°C and 310–528°C with peak maxima at 221 and 426°C at a heating rate of 10°C min<sup>-1</sup> in static air. When the atmosphere was changed to nitrogen the first exotherm was seen in the temperature range 202–226°C with peak maximum at 218°C. When the heating rate in static air was changed to 5 and 2°C min<sup>-1</sup> the first

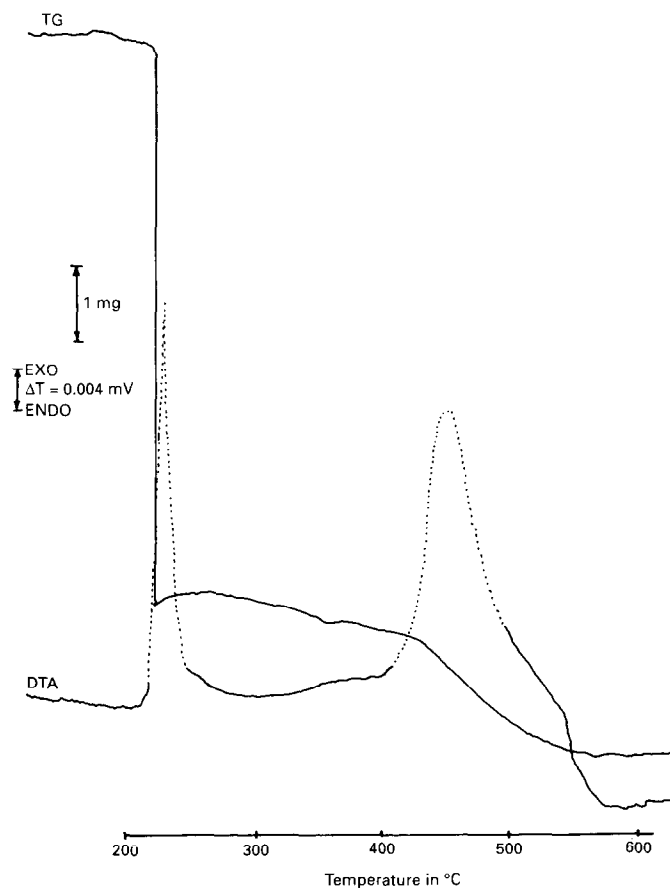


Fig. 2. TG–DTA of TNAD: sample mass, 10.0 mg; heating rate,  $10^{\circ}\text{C min}^{-1}$ ; reference, calcined alumina; atmosphere, static air.

exotherm was observed in the temperature ranges  $195\text{--}221^{\circ}\text{C}$  and  $183\text{--}217^{\circ}\text{C}$ , respectively.

DTA did not show any endothermic change before the onset of exothermic change indicating that the compound decomposed without melting.

### 3.3. Effect of additives

The effect of metal oxides/additives to the extent of 5% on the DTA profile corresponding to the initial thermolysis of TNAD, was recorded. From these curves  $\theta_i$ ,  $\theta_m$  and  $\theta_r$  have been evaluated and these values are arranged in increasing order of peak maximum temperature in Table 2.

It can be seen from Table 2 that all the metal oxides reduce the peak maximum temperature of TNAD, indicating that they accelerate the decomposition of TNAD; the effect of the majority of them is profound.

Table 2  
The effect of additives on the initial thermolysis of TNAD

Sample	Additive	Temperature of decomposition/°C		
		$\theta_i$	$\theta_m$	$\theta_f$
1	Copper chromite	174	177	195
2	Monobasic copper stearate	178	185	204
3	Magnesium oxide	183	190	210
4	Monobasic lead stearate	183	195	219
5	Cerium oxide	186	196	226
6	Zirconium dioxide	176	197	218
7	Lead monoxide	187	199	218
8	Titanium dioxide	187	200	218
9	Thorium oxide	181	201	220
10	Lanthanum oxide	188	202	211
11	Cobaltic oxide	193	202	221
12	Cupric oxide	186	204	221
13	Ferric oxide	191	204	221
14	Nickel oxide	205	207	231
15	TNAD	210	220	251

### 3.4. DSC studies

TG/DTA data were supplemented by DSC studies. The DSC trace at a heating rate of  $10^\circ\text{C min}^{-1}$  obtained with the sample encapsulated in an aluminium cup showed a sharp exothermic change. The onset of the exotherm was noticed at  $215^\circ\text{C}$  with the peak maximum at  $220^\circ\text{C}$ . This exothermic change was covered by an energy change of  $1142.3 \text{ J g}^{-1}$ .

### 3.5. Thermal decomposition kinetics

The kinetics [16] of the thermal decomposition of TNAD at different temperatures in the range  $185\text{--}200^\circ\text{C}$  under static air were studied by isothermal TG.

From the isothermal TG experiments the mass loss with respect to time was noted and  $\alpha$  the fraction decomposed at time  $t$  was evaluated.

The  $\alpha/t$  curve (Fig. 3) was analysed using various kinetic model functions for  $F(\alpha)$  tried in our studies [15] and the equations where close correlation was obtained are given in Table 3. However, the best fit with a correlation coefficient of 0.9859 was obtained for the three dimensional diffusion controlled equation  $[1 - (1 - \alpha)^{1/3}]^2$ . The rate constants were evaluated from the slopes of the plots of this equation at different temperatures studied. The Arrhenius plot gave an activation energy of  $156.48 \text{ kJ mol}^{-1}$  and a value for  $\log(A/\text{s}^{-1})$  of 13.77.

The correlation observed between the kinetics of initial thermolysis and the velocity of detonation has also been found to be valid in the case of TNAD (see fig. 9 in Ref. [15]).

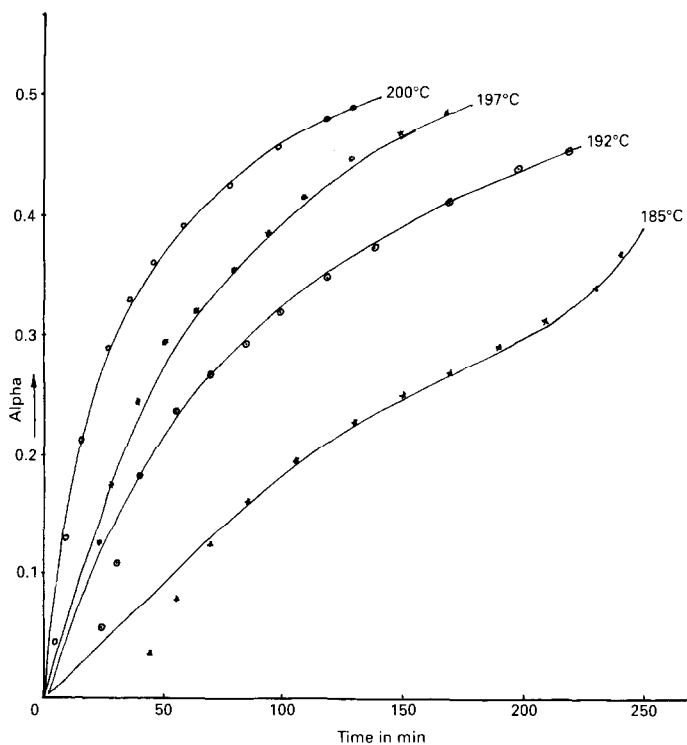


Fig. 3. Plot of  $\alpha/t$  for the thermal decomposition of TNAD (TG).

### 3.6. Evolved gas analysis

The obtained gaseous products of decomposition were identified using a dispersive ratio recording IR spectrophotometer (Perkin-Elmer Model 683) at a scanning rate of  $3 \text{ min scan}^{-1}$ . The sample was initially heated at a heating rate of  $10^\circ\text{C min}^{-1}$  up to  $190^\circ\text{C}$  and thereafter at  $5^\circ\text{C min}^{-1}$ . The spectra of the gaseous species obtained when the sample temperature was in the range  $210\text{--}225^\circ\text{C}$  are given and identified in Fig. 4.

Table 3  
Correlation coefficient  $R$  obtained for various  $F(\alpha)$  by isoTG

$F(\alpha)$	$R$ at isothermal temperatures of				$E/\text{kJ mol}^{-1}$	$\log(A/\text{s}^{-1})$
	$185^\circ\text{C}$	$192^\circ\text{C}$	$197^\circ\text{C}$	$200^\circ\text{C}$		
$\alpha^2$	0.9957	0.9873	0.9764	0.9369	134.59	12.11
$(1-\alpha)[\ln(1-\alpha)] + \alpha$	0.9941	0.9928	0.9847	0.9518	145.07	13.06
$(1-2/3\alpha) - (1-\alpha)^{2/3}$	0.9933	0.9942	0.9871	0.9566	148.87	12.86
$(1 - (1-\alpha)^{1/3})^2$	0.9914	0.9961	0.9909	0.9653	156.48	13.77
$[1/(1-\alpha)] - 1$	0.9827	0.9641	0.9626	0.9301	120.28	11.08

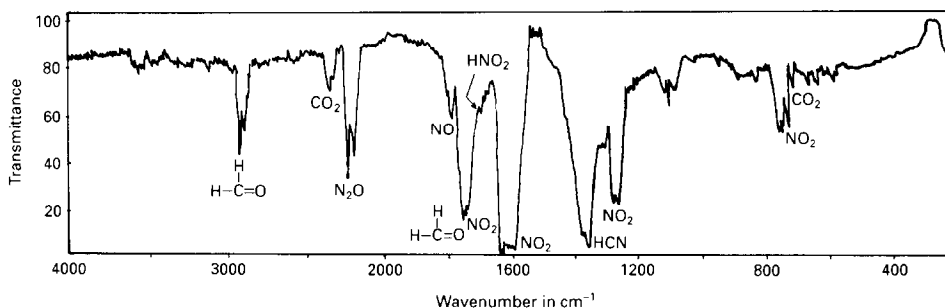


Fig. 4. IR spectra of gaseous decomposition products of TNAD.

### 3.7. Microscopic studies

In hot stage microscopy the crystals were seen to be of small needle shape and transparent. The transparency decreased with rise in temperature. Around 190°C the crystals turned blackish and evolution of brown gases was seen around 220°C.

## 4. Discussion

The TG/DTA results (Fig. 2) for TNAD indicate that the thermal decomposition of this compound proceeds in one main and another very slow stage. The decomposition involves about 92% loss in mass in the ranges 192–220°C and 220–512°C. The DTA curve shows two exothermic changes. The first exotherm seen in the temperature range 209–252°C is very sharp and corresponds to 75% loss in mass and the other seen in the temperature range 310–528°C corresponds to the slow mass change of 17% in TG. Isothermal TG changes indicate that the change in mass is up to 50% at 197°C in 220 min. These results conform with the reported findings of Brill and Oyumi [7] that TNAD turns brown around 217°C and deflagrates in the temperature range 227–247°C depending on sample size.

When the isothermal decomposition of TNAD was followed in KBr pellet or just mixed with KBr powder [15] it was observed that the intensity of the bands due to nitro and other groups decreased systematically. The loss of intensity due to nitro group was more pronounced than the intensities due to other groups. Development of new bands at 3400, 1750, 1680, 1530 and 1380  $\text{cm}^{-1}$  was noticed in the loose mix method. In the KBr pellet (Fig. 5) in addition to these bands new bands at 2340 and 2220  $\text{cm}^{-1}$  were also noticed. In evolved gas analysis nitrogen dioxide, formaldehyde, carbon dioxide and nitrous oxide were the major components, while nitric oxide, carbon monoxide and hydrogen cyanide were the minor gaseous products identified by IR.

The spectra of the residue obtained at 50% loss in mass in the isothermal TG experiment showed development of new bands at 1750, 1680 and 1530  $\text{cm}^{-1}$ . The observation of a large quantity of  $\text{NO}_2$  in the evolved gas analysis and the observed

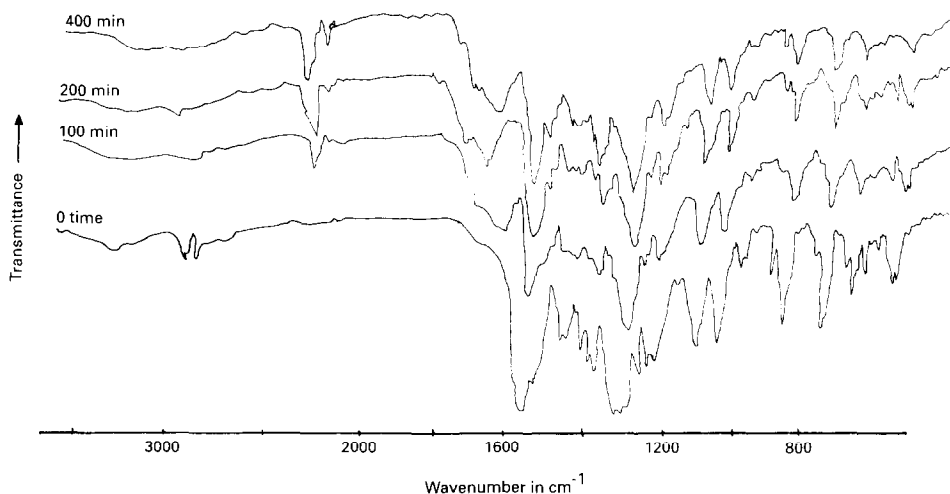


Fig. 5. IR spectra of TNAD at 185°C in KBr pellet.

preferential loss of band intensity due to the  $\text{NO}_2$  group permits us to conclude that N–N bond cleavage may be the initial thermolysis pathway in TNAD.

The bands at  $1680\text{ cm}^{-1}$  are characteristic of a C=N group. The band at  $1750\text{ cm}^{-1}$  can be assigned to a carbonyl group. The bands at  $2340$  and  $2220\text{ cm}^{-1}$  could be ascribed as before to trapped  $\text{CO}_2$  ( $2340\text{ cm}^{-1}$ ) and  $\text{N}_2\text{O}$  ( $2220\text{ cm}^{-1}$ ) in the matrix while the band at  $3400\text{ cm}^{-1}$  could arise from an amino linkage.

Brill and Oyumi [7], who have investigated the evolved gases from the thermal decomposition of TNAD, observed that considerable amounts of HONO and  $\text{NO}_2$  are produced at lower heating rates. They further showed that the ratio of HONO/ $\text{NO}_2$  obtained was higher at high pressures than at low pressures [7]. According to them, at higher pressures it is likely that the initially formed  $\text{NO}_2$  is unable to diffuse and get engaged in further reactions with the condensed phase producing HONO, whereas at lower pressures the  $\text{NO}_2$  cleaved can easily diffuse through. Thus the HONO formed may be due to the adventitious contact of the  $\text{NO}_2$  formed with the ring hydrogen atom. According to Brill and Oyumi [7], in nitramines the formation of HONO is advanced with larger H/ $\text{NO}_2$  ratios and it is not a primary decomposition product; the bands at  $1696\text{ cm}^{-1}$  and around  $1300\text{ cm}^{-1}$  are assignable to HONO. As mentioned above in the present study only weak bands were noticed, perhaps due to the reported instability of HONO. However the formation of HONO can be rationalised from the observation of a new band at  $1680\text{ cm}^{-1}$  ascribable to the C=N group. This group probably has its origin in the abstraction of a hydrogen atom from the ring by the initially cleaved  $\text{NO}_2$ , as summarised in Fig. 6. After the initial cleavage has taken place the specified secondary reactions can account for the other products observed in IR studies.

Murray et al. [17,18], using an ab initio self consistent field (SCF) molecular orbital approach in conjunction with the isodesmic reaction procedure, have reported some anomalous energy effects in nitramines. These molecules have been



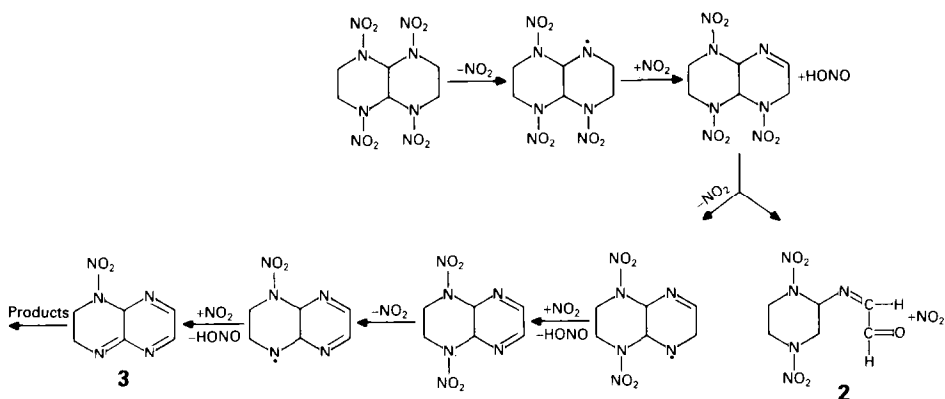


Fig. 6. Proposed mode of thermal decomposition of TNAD.

found to be significantly stable, which they attributed to the conjugation of the nitrogen lone pairs. These lone pairs of electrons presumably appear to be delocalised to some extent in the same bond framework. The stabilisation increases with the number of nitrogen atoms in cyclic systems, particularly when the rings are fused. The magnitude of the most negative electrostatic potentials of the nitrogens can be considered to be indicative of the degrees of delocalisation of the nitrogen lone pairs, and decreases as the stability increases. In aza cyclic systems the introduction of nitro rings also has an overall stabilising effect due to further delocalisation of electrons, reflecting the strong electron withdrawing power of the nitro group.

The intermediate **2** (Fig. 6) can give the band at  $1750\text{ cm}^{-1}$ , while that marked **3** can give rise to the band at  $1530\text{ cm}^{-1}$  which is characteristic of a conjugated ring system. It is most likely that the mechanism suggested by Cosgrove and Owen [19] operates like a competitive secondary reaction because we have been able to detect  $\text{N}_2\text{O}$  as a product in evolved gas analysis.

Melius [20] has recently applied thermochemical modelling to decompositions of energetic materials and has shown that in RDX and HMX the weakest bond is  $\text{N}-\text{NO}_2$ . The bond breaking energy for this  $\text{N}-\text{N}$  bond in RDX is  $205.0\text{ kJ mol}^{-1}$  and in HMX it is  $206.0\text{ kJ mol}^{-1}$ , but the  $\text{C}-\text{N}$  and  $\text{C}-\text{H}$  bonds are significantly stronger. The bond breaking energies for the  $\text{C}-\text{N}$  and  $\text{C}-\text{H}$  bonds are  $375.0\text{ kJ mol}^{-1}$  and  $395.8\text{ kJ mol}^{-1}$ , respectively, in HMX and of similar order in RDX. However, after the rupture of the  $\text{NO}_2$  group, the resulting second nearest neighbour bond breaking energies become very weak; for example, the  $\text{C}-\text{N}$  bond breaking energy is only  $75.6\text{ kJ mol}^{-1}$  in HMX. Therefore in the unimolecular decomposition of RDX and HMX the order in which the bonds are broken is  $\text{N}-\text{N}$  followed by  $\text{C}-\text{N}$ .

The  $E$  value [21] reported for RDX by the isothermal gas evolution method [22] is  $198.6\text{ kJ mol}^{-1}$  ( $213\text{--}299^\circ\text{C}$ ); from mass spectroscopic studies [23,24] it is  $188.1\text{ kJ mol}^{-1}$ . The  $E$  value reported for HMX is  $220.3\text{ kJ mol}^{-1}$  ( $271\text{--}314^\circ\text{C}$ ) by the isothermal gas evolution method [22] and  $204.8\text{ kJ mol}^{-1}$  by the isothermal mass

loss method [25]. The  $E$  value obtained in the present study suits the mechanism proposed [15,26,27] reasonably well and is consistent with those for RDX and HMX when the expected weaker N–N bond dissociation energy and the lower temperature of decomposition in TNAD are taken into account. It is possible thereby to infer that the N–NO<sub>2</sub> bond cleavage is the primary step in the thermal decomposition of TNAD.

## References

- [1] G.P. Sollot and E.E. Gilbert, *J. Org. Chem.*, 45 (1980) 5405.
- [2] P.E. Eaton and B.K. Ravishankar, *J. Org. Chem.*, 49 (1984) 185.
- [3] R.L. Willer, *Propellants Explos. Pyrotech.*, 8 (1983) 65.
- [4] M.M. Stinecipher and L.A. Stretz, 8th Int. Symp. on Detonation, Albuquerque, NM, 15–19 July, 1985, vol. 2, p. 608.
- [5] M. Farber and R.D. Srivastava, 16th JANNAF Combustion Meeting, Monterey, CA, CPIA Publication No. 308, Dec. 1979, p. 59.
- [6] R. Shaw and F.E. Walker, *J. Phys. Chem.*, 81 (1977) 2572.
- [7] T.B. Brill and Y. Oyumi, *J. Phys. Chem.*, 90 (1986) 6848.
- [8] Y. Oyumi and T.B. Brill, *Combust. Flame*, 68 (1987) 209.
- [9] S. Zeman, M. Dimun and S. Truchlik, *Thermochim. Acta*, 78 (1984) 181.
- [10] P. Politzer, J.S. Murray, P. Lane, P. Sjoberg and H.G. Adolph, *Chem. Phys. Lett.*, 181(1) (1991) 78.
- [11] J.S. Murray, P.C. Redfern, J.M. Seminario and P. Politzer, *J. Phys. Chem.*, 94(6) (1990) 2320.
- [12] P. De, L.G. Jose and J. Ciller, *Propellants Explos. Pyrotech.*, 18(1) (1993) 33.
- [13] Y. Yinon, NATO ASI Ser. C, *Chem. Phys. Energ. Mater*, 309 (1990) 695.
- [14] Yu.Yu. Nikishev, I.S. Saifullin and I.F. Falyakhov, *Kinet. Katal.*, 32(3) (1991) 749.
- [15] K.V. Prabhakaran, N.M. Bhide and E.M. Kurian, *Thermochim. Acta*, 220 (1993) 169.
- [16] E.M. Kurian, *J. Therm. Anal.*, 35 (1989) 1111.
- [17] J.S. Murray and P. Politzer, in S.N. Bulusu (Ed.), *Chemistry and Physics of Energetic Materials*, Kluwer Academic, Boston, 1990, pp. 157, 175.
- [18] J.S. Murray, P.C. Redfern, P. Lane, P. Politzer and R.L. Willer, *J. Mol. Struct. (Thermochem)*, 66(3/4) (1990) 177.
- [19] J.D. Cosgrove and A.J. Owen, *Combust. Flame*, 22 (1974) 13.
- [20] C.F. Melius, in S.N. Bulusu (Ed.), *Chemistry and Physics of Energetic Materials*, Kluwer Academic, Boston, 1990, p. 43.
- [21] T.L. Boggs, in K.K. Kuo and M. Summerfield, *Fundamentals of Solid Propellant Combustion*, AIAA, New York, 1984, p. 121.
- [22] A.J.B. Robertson, *Trans. Faraday Soc.*, 45 (1949) 85.
- [23] B. Suryanarayana, R.J. Graybush and J.R. Autera, *Chem. Ind. (London)*, 52 (1967) 2177.
- [24] B. Suryanarayana and R.J. Graybust, *Proc. 39th Congress on Industrial Chemistry*, Brussels, Belgium, 1966.
- [25] K.J. Kraeutle, 18th JANNAF Combustion Meeting, Pasadena, CA, 19–23 October 1981, CPIA Publication No. 347, Nov. 1981, p. 383.
- [26] K.V. Prabhakaran, S.R. Naidu and E.M. Kurian, *Thermochim. Acta*, 241 (1994) 199.
- [27] S.R. Naidu, N.M. Bhide, K.V. Prabhakaran and E.M. Kurian, *J. Therm. Anal.*, in press.